The Glaciolacustrine Sediment Record of Cariboo Lake: Implications for Holocene Fluvial and Glacial Watershed Dynamics in Eastern British Columbia, Canada

2022-10-06

Alexander Cebulski[1] (ORCID ID - 0000-0001-7910-5056), Joseph Desloges[2] (ORCID ID - 0000-0001-8446-3034)

[1]Department of Geography and Planning, University of Saskatchewan, Canada

[1]Department of Geography and Department of Earth Sciences, University of Toronto, Canada

Abstract: Cariboo Lake is situated in a mountainous region of British Columbia Canada and is representative of environments transitioning from semi-arid interior climates to glaciated high mountain regions to the east. Sub-bottom acoustic transects and short and long sediment cores are analyzed to present a high-resolution record of sediment accumulation over the Holocene. Acoustically penetrable sediment reaches a maximum thickness of 35 m in deep parts of the lake, representing deglacial and Holocene accumulation. A transition from massive to well-layered sediments is observed in the sub-bottom acoustic record during final phases of valley deglaciation in the region (ca. 10.5-9 ka BP). Fine clastic sediments produced from the glaciated headwaters are delivered by Cariboo River as over-flow currents into the lake which produce bimodal rhythmic layering of silt and clay sediments. Laminae couplets are inferred to be deposited annually according to two AMS radiocarbon dates and a varve counting chronology. Two long cores, 2.9 and 3.8 m in length, were selected for analysis with estimated basal dates of ~2 ka BP. The accumulation of sediment into Cariboo Lake shows above average sediment accumulation rates between 0-700CE and 1500-2017CE which are coincident with cool temperatures and peak glacier extents. The sediment chronology presented in this study contributes to the existing body of knowledge of lake sediment accumulation and Holocene watershed activity for this transitional climate region of western Canada.

Keywords: Lake, Sediment, Holocene, Acoustic records, Varve, Climate proxy, British Columbia

---

Contents

1 Introduction

Environmental proxies that extend back beyond the modern observable record are crucial to understanding earth system processes (Huber and Knutti, 2012; Nelson et al., 2016; Turney et al., 2019). Proxy reconstructions at the sub-annual scale (e.g. ice cores, tree rings, and corals), to multi-decadal scales (e.g. sediments, pollen, boreholes) have proven useful in describing past environmental conditions across the globe (Masson-Delmotte et al., 2013). Sedimentary sequences collected from climate sensitive glaciated watersheds have been important in contributing to the regional understanding of climate and hydrologic variability over the Holocene. Research by Neukom et al. (2019) have utilized sedimentary sequences as part of larger paleolimnological collections to provide global reconstructions of temperature variability over the last 2000 years. In the western Cordillera of Canada, recovered sedimentary sequences have been collected in the Coast Mountains (Menounos and Clague, 2008), St. Elias Mountains (Crookshanks and Gilbert, 2008), Monashee Mountains (Hodder et al., 2006), and Rocky Mountains (Desloges, 1999; Dirszowsky and Desloges, 1997; Leonard, 1986). A study of Quesnel Lake (272 km^2), nearby the study area examined here, by Gilbert and Desloges (2012) found deglacial, and the very earliest Holocene, sediment infills to be high at around 10.4 ka BP, declining significantly at around 8.4 ka BP. Trends in Quesnel Lake sediment characteristics during the Holocene were not detectable as accumulation rates were very low in the areas of the lake that could be sampled. Quesnel Lake is very large relative to the contributing watershed and therefore the sediment system is much less sensitive to climate variability. Previous studies on lakes in smaller watersheds with significant glacier cover have had greater success relating lake bottom sediment archives (e.g. varves) to changes in regional temperature, precipitation patterns, and glacier extent over the Holocene (Desloges, 1999; Hodder et al., 2006; Menounos et al., 2006). However, when sediment inputs are high due to high flows and/or extensive glacier melt, this can limit the ability to sample the very thick accumulations and reduces temporal coverage (e.g. Desloges and Gilbert, 1994). Lakes that are more distal from glacier activity typically have relatively lower sediment inputs, due to the upstream filtering of rivers and/or lakes which limits the coarser fraction of sediment but still allow some input of the fine fraction (Hodder et al., 2007). The effect of this filtering effect on the climate and hydrology signal may contribute to a weak signal to noise ratio (Jerolmack and Paola, 2010). To fill in the gap between high resolution and long temporal coverage (entire Holocene thick sequences), the study here uses Cariboo Lake (10 km^2) draining 3244 km^2 in the Cariboo Mountains of eastern-central British Columbia.

This study aims to present a new record of Holocene hydro-climatic variability using lake bottom sediment records recovered using sub-bottom acoustic methods and long sediments cores. To determine if Cariboo Lake contains a record of regional temperature and precipitation variability, the relative role of sediment inputs is assessed. This includes sources from the upstream Cariboo River, controlled by watershed wide trends in temperature and precipitation, and inputs from smaller unglaciated watersheds that border the lake.

The purpose of this research is to 1) establish an understanding of the mechanisms that control the delivery and deposition of the fine sediment fraction to Cariboo Lake, 2) to reconstruct the highest resolution and longest term sediment accumulation record possible for this area of British Columbia, 3) compare and contrast the accumulation record in this transitional (semi-arid to glaciated mountainous) lake system with existing sedimentary sequences in western Canada and regional climate proxies.

2 Study Area

Cariboo Lake is located in the northern foothills of the Columbia Mountains, 85 km northeast of Williams Lake, British Columbia (Figure 1). The lake receives runoff from an area of 3244 km^2, and the watershed relief ranges from 2600 m asl. in the eastern headwaters to 600 m asl. at the western Cariboo Lake outlet. The west to east, 90 km long watershed spans climate ranging from 1370 mm/yr in the headwaters to 477 mm/yr at the semi-arid outlet to the lake. The area of Cariboo Lake is 10 km^2 resulting in a lake area-to-watershed area ratio of 0.3%. The Cariboo Lake watershed has 64 km^2 of permanent ice cover which covers

2% of the total watershed (Bolch and Bolch, 2008). The most extensive glaciated terrain is proximal to Mt. Lunn roughly 60 km upstream of Cariboo Lake (Figure 1).

The Cariboo River, draining into the east margin of the lake, is the main source of sediment. The lake is separated into two basins, by a large alluvial ban building cross-valley from Keithley Creek (Figure 2). The upstream basin is 8 km^2 and is referred to here as the main Cariboo Lake basin. The downstream basin, referred to here as the Keithley Creek sub-basin, is 2 km^2. The bathymetry of the lake reaches a maximum depth of over 50 m in two deep holes within the central part of the main Cariboo Lake basin. These deep holes provide some evidence of past glacial scouring.

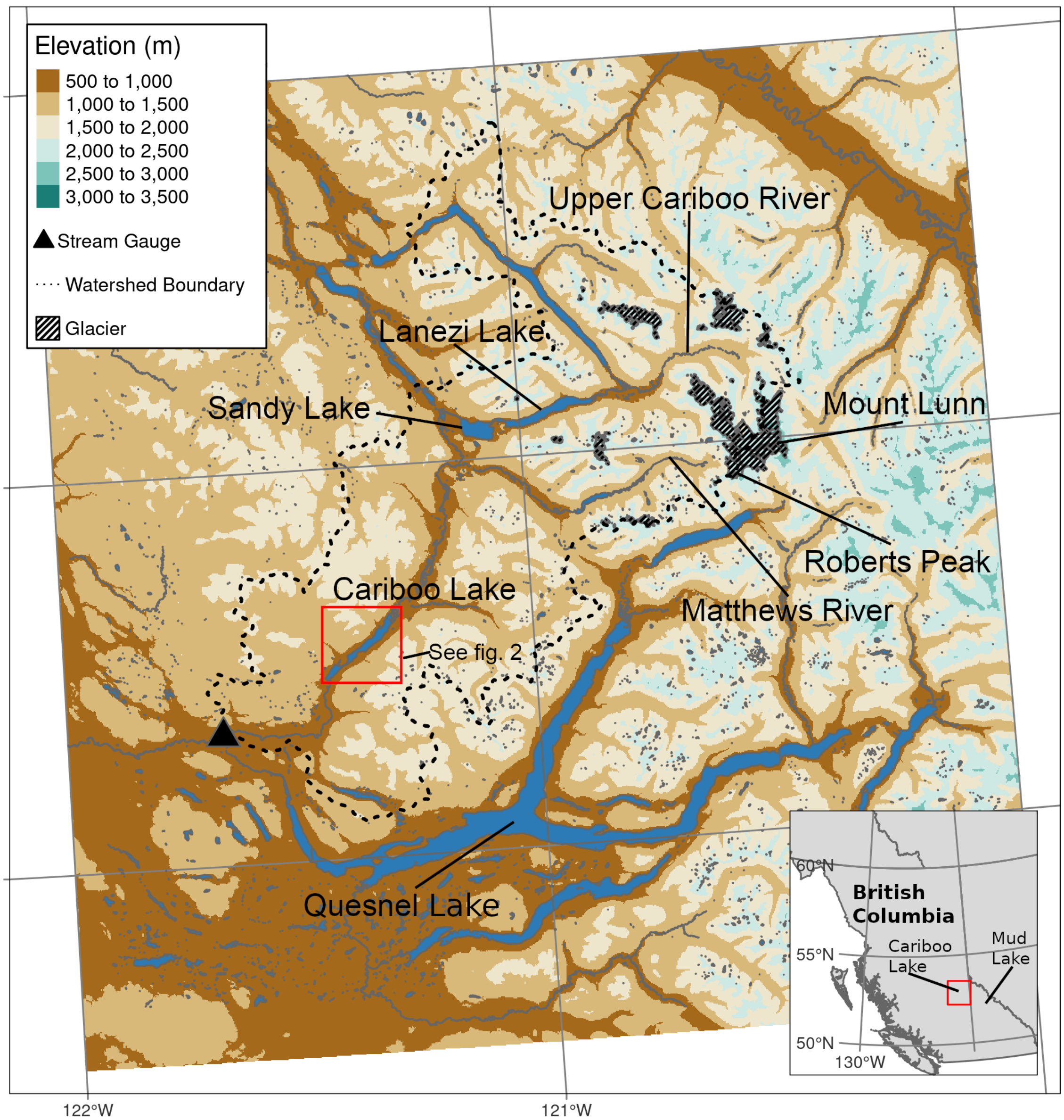

Figure 1: Map of the Cariboo Lake basin. Inset map shows the location of the Cariboo Lake basin within British Columbia relative to the Mud Lake basin from the Hodder et. al, (2006) study. See Figure 2 for detailed map of Cariboo Lake.

Sediment connectivity to headwater glaciers along the Cariboo River is limited due to lake filtering by Lanezi and Sandy lake (Figure 1). Lanezi Lake is a deep fjord-like lake with a bathymetry reaching a maximum

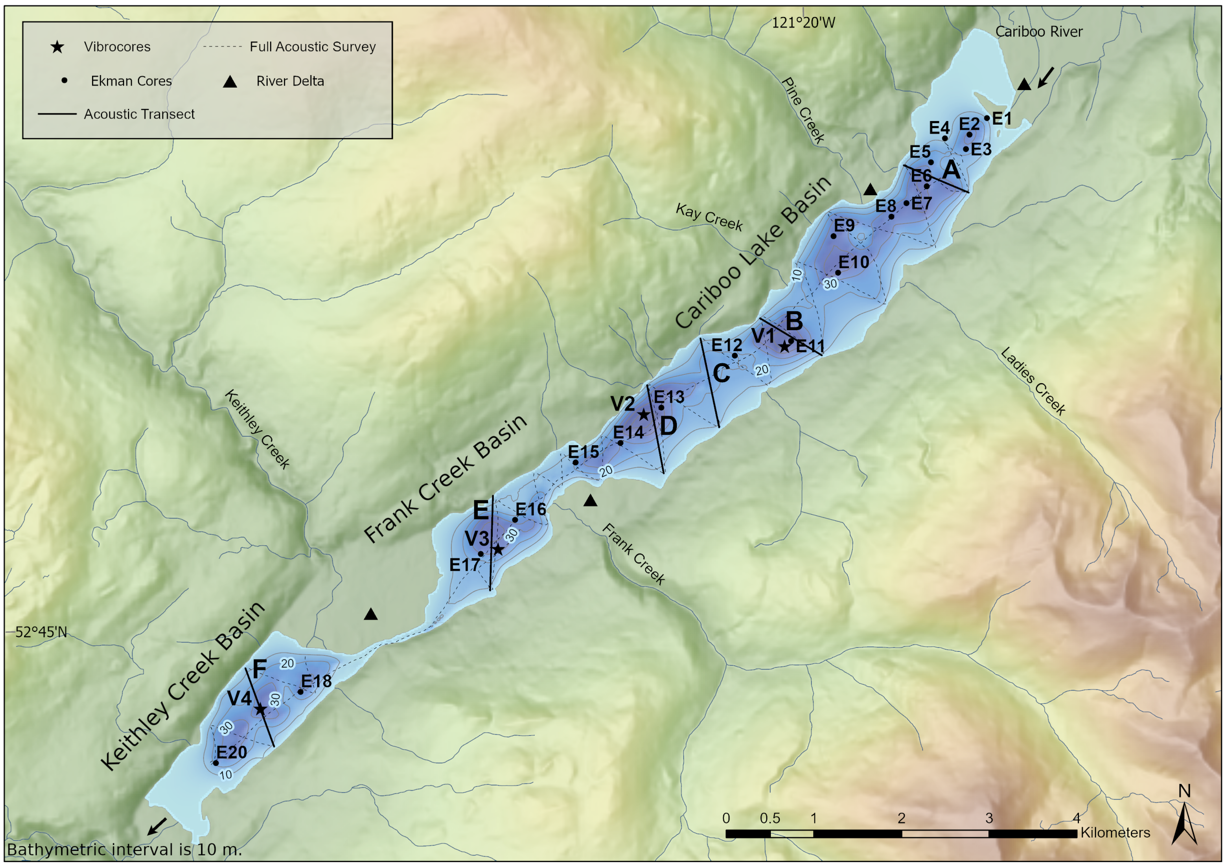

Figure 2: Map of the Cariboo Lake bathymetry and coring locations. Bathymetric interval is 10 m. Acoustic transects selected for analysis are shown with a black solid line and labeled A, B, C, D, E and F. Fan deltas mentioned in the text are represented by black triangles and are referenced to by the upstream creek (i.e. Frank Creek Delta is the triangle below Frank Creek). The Frank Creek fan delta separates the main Cariboo Lake and Frank Creek sub-basins. The Keithley Creek fan delta separates the Frank Creek and Keithley Creek sub-basins.

depth of 170 m. Sandy Lake is much shallower reaching a maximum depth of 6 m. The Matthews River, which meets the Cariboo River just below Lanezi Lake provides a less filtered connection to meltwater sources draining several alpine glaciers including the largest area of ice (10 km^2) in the Cariboo Lake watershed, proximal to Roberts Peak (Figure 1).

3 Methods

3.1 Field Methods

A field campaign was conducted during the summer of 2017 to collect sub-bottom acoustic soundings, dredge samples, and sediment cores. Thirty-four km of sub-bottom acoustic soundings were collected across Cariboo Lake using a 10 kHz StrataBox 3510 HD. An Ekman dredge was used to collect 20 samples from the lake bottom, each yielding ~730 cm^3 of surficial sediment. The dredge samples were sub-sampled in the field using an 80 mm diameter PVC cylinder pushed into the block of sediment. This resulted in 20 short cores each containing about 450 cm^3 of sediment. The remaining sediment not captured in the PVC cylinder was kept as a bulk sediment sample. Four long sediment cores (V1-V4) were collected using a Rossfelder submersible vibracorer with a 6 m long 70 mm diameter aluminum pipe. The Ekman short cores and the long vibracores were split longitudinally with one half preserved as an archive and the other as a working half. The working half samples were prepared for imaging by scraping the core parallel to the sediment laminae to create a flat surface which showed the sediment stratigraphy. The stratigraphy of long cores V1 and V2 were best preserved and were selected for detailed analysis.

3.2 Laboratory Methods

The cores and short cores were analyzed for laminae thickness, organic content, and particle size. Long cores V1 and V2 were subsampled with 2 cm^3 of sediment extracted at a 5 cm interval, with additional samples taken within stratigraphic breaks. Laminae couplets observed on the working cores were digitally counted and measured for thickness using the ImageJ software, by Schneider et al. (2012). Organic content was determined by loss-on-ignition analysis (550 °C) following methods in Smith (2003). Samples were first weighed to provide an initial wet weight, then dried at 60 °C and weighed again after oven drying. The samples were then placed in a furnace at 550 °C for 2.5 hours and weighed a third time. Grain size analysis was conducted using a Mastersizer Particle Size Analyzer 3000. Samples were prepared following methods by Gray et al. (2010) to remove the fine fraction of particles from organic material. This involved a removal of organic material using three sequential alloquots of 20% H_20_2 until the sample stopped reacting. To prevent flocculation of sediment grains the samples were dispersed in 0.05% solution of Calgon for 24 hours. Grain size was measured three times for each sample, resulting in an average standard deviation of +/- 0.01 µm. The chronology of both vibra cores was reconstructed using AMS ^{14}C dating of three wood fragments (analyzed at the André E. Lalonde AMS Laboratory at the University of Ottawa) and a chronology derived from laminae (couplet) counting on working core images.

4 Results

4.1 Sub-bottom Acoustics

Acoustic stratigraphy from six selected transects (see locations in Figure 2) reveal the range of morphologies and character of sedimentary deposits in Cariboo Lake (Figure 3). Acoustic penetration is limited in transects A and E by coarser sediments proximal to river fan-deltas across Cariboo Lake (see triangle symbols in Figure 2 for fan-delta locations). Acoustic signal penetration, resolution and distinctive acoustic layering improves significantly along the thalweg of the lake bottom away from the main Cariboo River delta and in cross-lake transects more distal from the valley-side fan-deltas. Cross-hatching is observed over most of the acoustic record due to errant electrical interference from the research vessel that could not be resolved. However, the interference does not affect the overall quality of the acoustic results in the six selected transects (Figure 3, A-F).

Transect A, one kilometer southwest of the headwater Cariboo River delta, has a strong acoustic reflector at the sediment-water interface indicating the presence of coarser-grained material on the lakebed (Figure 3, A). Grab samples on this transect show a high fraction of sandy materials which act as an acoustic mask limiting the penetration of the acoustic signal to a depth of 1-2 m. An acoustic multiple (echo) is observed 45 m below the sediment surface caused by the limited penetration at the surface (Figure 3, A - i).

Acoustically penetrable, well-layered sediment is observed 3.5 km from the Cariboo River delta in transect B (Figure 3, B). This site is proximal to long core V1. Acoustic reflectors with 1-2 m separation lie conformably over a hummocky basement which is observed on the south side of the transect (Figure 3, B - i). The acoustic basement drops off below the observable record near the south channel-like depression. Well structured layering extends across the south side of the transect but pinches out towards the north shore (Figure 3, B, C & D). On the south side of the transect, the thickness of the well structured layering ranges from 10 to 20 m. Underlying the layered sediments is a more massively layered facies which ranges from 12 to 25 m thick before the record is cut off.

Acoustic penetration increases 4.5 km from the Cariboo River delta at transect C (Figure 3, C). The acoustic record along this transect reaches a maximum sediment thickness of 35 m in two troughs, the maximum thickness of surficial sediments observed across Cariboo Lake in this study. The acoustic basement is considered to be either bedrock or coarse-grained glacial sediment from the Last Glacial Maximum (Figure 3, C – i). Two sediment facies are observed across this transect based on geometry and the strength and continuity of reflectors. Some disruption of these facies is caused by slumping of side slopes (e.g. north end of transect C). The lower unit, facies A, has a thickness of ~ 12 m along undisturbed sections (Figure 3, C) and is more massive to weakly acoustically layered. The contact with overlying sediment above facies A appears to be conformable at the south end and middle of the transect but unconformable in other places. The unconformities are most apparent in the two sharp crested v-notch channels at the middle of the transect. These channels are a continuation of those noted in transect B. These are inferred to be scour channels formed by erosive, higher energy, turbidity currents that probably date to deglaciation of the lake basin. The lack of numerous layers and generally lighter grey tone in facies A indicates a somewhat higher energy and more rapid deposition of coarser lacustrine sediment. Facies B begins with high-amplitude parallel reflectors with 2-3 m separation and conforms well with facies A below (Figure 3, C). Facies B has a thickness of ~ 10 m along undisturbed sections and deepens to a maximum of 13 m within the scour channels (Figure 3, C - ii & iii). The strength of reflectors in facies B are stronger and more numerous than those in facies A indicating more frequent events of lower overall magnitude during this time. The strength of reflectors gradually decreases moving upwards and spacing thins to sub metre thickness near the surface. The gradual decrease in reflectance is interrupted by a strong reflector at the top of facies B along the sediment-water interface. The two buried troughs in transect C (Figure 3, C - ii, iii) are significant and best expressed in this area of the lake. The north trough (ii) appears to be a depression that was continuously infilled by facies A and then B. Hence it most likely represents an older pre-existing feature. The sediments in the southern trough (iii) are interesting in that a wedge of sediment infill seems to be an unconformable deposit with both facies B below and facies A above. It is likely that an erosional channel developed after or in the later stages of facies A deposition which infilled the wedge. Sedimentation of the wedge was then truncated by the onset of the facies B sediment. While the two troughs might have been active at the same time during deglaciation, only the southern trough was reactivated at a later time and infilled with sediment prior to the onset of facies B deposition.

Transect D, to the northeast of the Frank Creek delta has well-layered sediments in the top 5-10 m and transitions to poor acoustic penetration below this (Figure 3, D). The parallel reflectors observed in the uppermost sediment layers of transect D have a thickness of 2-3 m and have a higher amplitude compared to facies B in transect C. Some slumping of sidewall sediments is observed on the south sidewall (Figure 3, D).

Southwest of the Frank Creek fan-delta, acoustic reflectors along transect E show a decline in reflectance and a decrease in layer thickness to < 1 m. Acoustic masking from coarse grained sediment occurs at depths

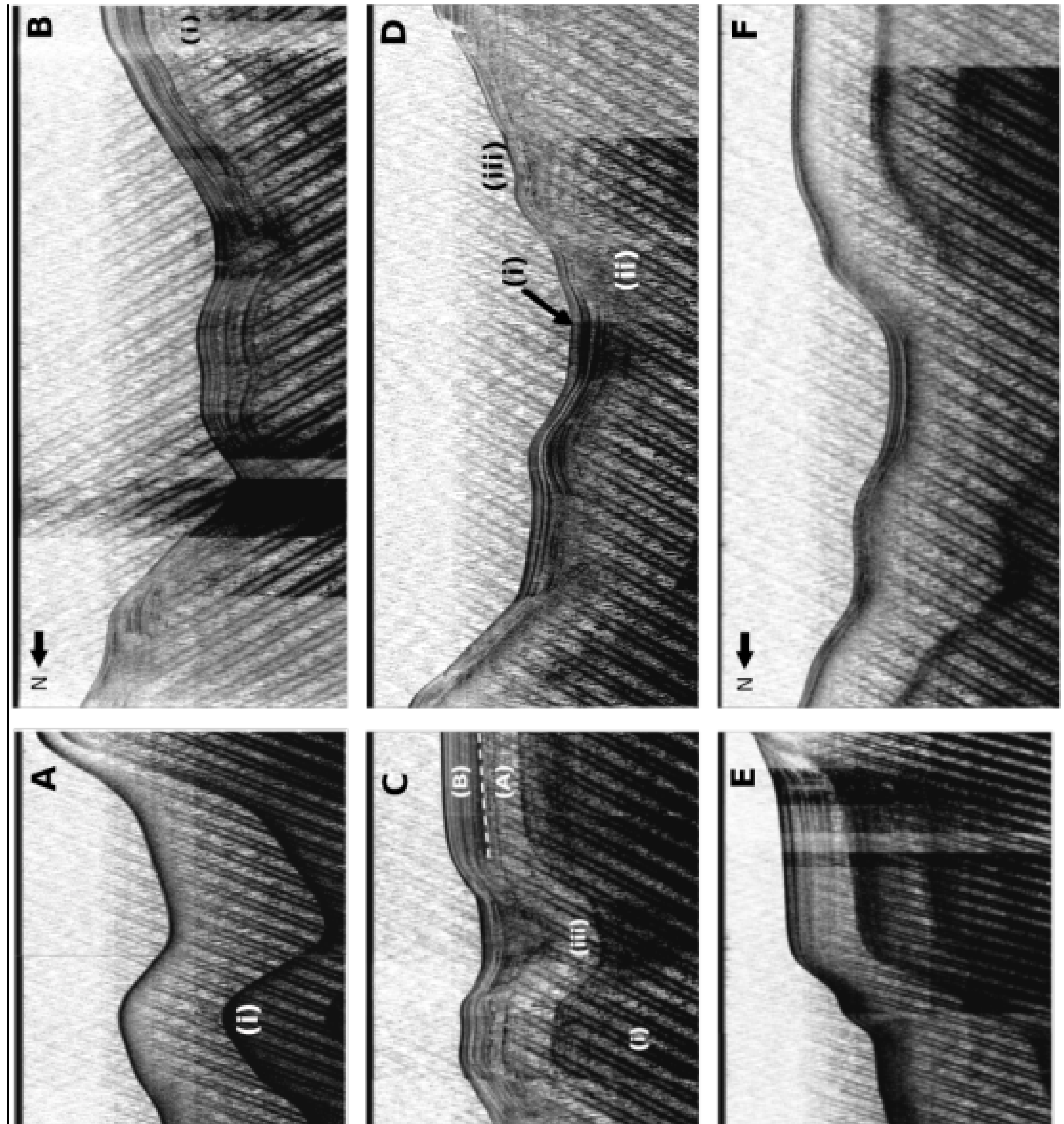

Figure 3: Panel of six selected sub-bottom acoustic transects A, B, C, D, E, and F. All transects are looking up-lake, see Figure 2 for location of each transect. Transect A and B: Acoustic echo (multiple) is denoted by (i). Transect C: (i) denotes inferred bedrock or coarse late-glacial material. (ii) and (iii) are v-notch scour channels. (A) and (B) are sediment facies. Transect D: Scour channels are denoted by (i) and (ii). Slumping is observed at (iii).

of 2-4 m along the south margin (Figure 3, E). Total sediment thickness of finer, acoustically well-layered material along the north bench is significant approaching 10 m. The sedimentary environment southwest of the Frank Creek delta is different to transects northeast of the delta. The profile suggests that much of the suspended sediment transported from the upper lake does not make it past the shallow lake depths (< 20 m) of the sill at the Frank Creek fan-delta apart from the northern most part of the transect. So, coarser sediment from the Frank Creek fan-delta dominates the south side of the transect and fine sediment deposition is restricted, or forced, to the north side. The Coriolis effect may enhance this as suspended sediments are deflected to the right as they enter Cariboo Lake from Frank Creek.

Similar to the Frank Creek fan-delta, the very shallow sill of less than 2 m opposite the Keithley Creek prograding fan-delta significantly reduces sediment connectivity to the main Cariboo Lake basin (see triangle proximal to Keithley Creek in Figure 2). Transect F, located close to the centre of the Keithley Creek sub-basin shows a maximum observable sediment thickness of 4 m concentrated in the basin thalweg (Figure 3). Below this there is acoustic masking by coarser sediment. The acoustic reflectors within the top 4 m of transect F are acoustically penetrable, well layered and are conformable to the basin morphology. These reflectors are of higher amplitude compared to those in transect E and are thicker at 1-2 m. This suggests that significant amounts of coarse-grained sediments are found in this part of the lake, likely originating from the high energy Keithley Creek drainage basin. Fine faction sediments from the main Cariboo Lake are expected to make up a small percentage as transport into this sub-basin is limited by up-lake storage, filtering and hypopycnal overpassing.

4.2 Spatial Trends in Surficial Sediment

Twenty surficial sediment cores ranging from 6-12 cm thick were analyzed for grain size, laminae thickness, and organic content. These samples were collected following a longitudinal transect down Cariboo Lake and indicate how sediment flux varies with distance from the Cariboo River delta (see Figure 2, for sampling locations). The D_{50} grain size follows a steep decline from 89.9 µm, 300 m from the delta, to 31.3 µm 550 m from the Cariboo River delta (Figure 4, A). The decline in D_{90} grain size follows a more pronounced decline, while the D_{10} remains largely unchanged. This suggests that larger sand-sized sediments are sensitive to distance from fan deltas, while smaller silt- and clay-sized sediments are less sensitive. The decrease in D_{50} and D_{90} grain size generally continues further down-lake with the exception of samples proximal to valley-side fan-deltas. A small increase in D_{50} is observed proximal to the Pine Creek fan-delta from a low of 21.5 µm at 1.1 km and up to 28.2 µm 1.83 km from the main Cariboo River delta (Figure 4, A). At distances greater than 2 km from the Cariboo River delta the fraction of silt-sized sediments remains at over 80 %, aside from core E16 which is near the Frank Creek fan-delta. Proximal to the Frank Creek fan-delta the D_{50} grain size nearly doubles in size from 7.92 µm at 6.4 km to 15.1 µm at 7.35 km from the Cariboo River delta. In the Keithley Creek sub-basin the D_{50} grain size has an average grain size of 15.9 µm (n = 3) and the composition of sediment is 4.0% clay, 85.8% silt, and 10.2% sand (Figure 4, A).

Proximal to the Cariboo River delta (< 500 m) the structure of the surficial sediments exhibits massive layering, erosive contacts and the fraction of sand grains in these samples is greater than 60%. A sand-bed with a thickness of 1 cm is observed in the bulk sample closest to the Cariboo River delta (Figure 5, A). In the main Cariboo River basin, the most well-preserved core (E13) was taken 5.24 km from the Cariboo River delta, proximal to long core V2, in the deepest part at a depth of 40 m. Sediment here shows rhythmic lamination (Figure 5, B).

Sediment cores E9-E15 and E18-E20, retrieved from areas in Cariboo Lake that are distal from river deltas and have lake depths of 30-50 m, have a high fraction of silt and clay sediment and exhibit a sequence of fine-grained dark layers followed by coarse-grained light layers (Figure 5, B & C). The thickness of sediment laminae couplets within these surface cores demonstrate a gradual decreasing trend with distance down-lake from the Cariboo River delta (Figure 4, B). Maximum couplet thickness has an average of 4.7 mm (n = 6) in the Cariboo River basin and 7.9 mm (n = 3) in the Keithley Creek sub-basin. In the Cariboo River basin, maximum couplet thickness decreases by 0.62 mm/km and by 2.17 mm/km in the Keithley Creek sub-basin with distance down-lake (Figure 4, B). This decrease in couplet thickness with distance from the main contributing delta's is attributed to the Cariboo River being the main source of sediment into Cariboo

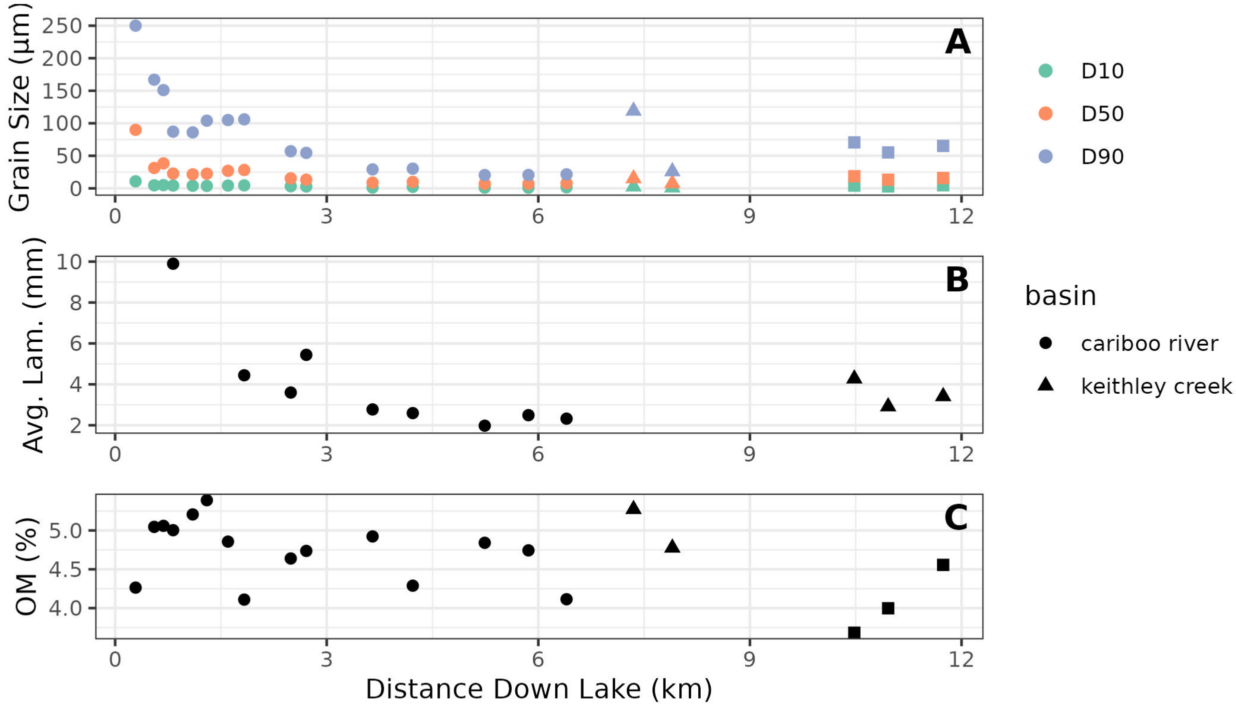

Figure 4: Sediment characteristics from the Ekman surficial bulk samples with distance down lake from the Cariboo River input to Cariboo Lake. Top panel A is the D 50 (µm) grain size, middle panel B is the mean laminae thickness (mm), and the bottom panel C is percent organic matter content (OM).

Lake as sediment flux typically declines with distance from the primary sediment source. The decline in thickness is more rapid in the Keithley Creek sub-basin is likely due to additional local inputs of coarser grained sediment coming from the Keithley Creek tributary.

Trends in percent organic matter (OM) of surficial sediment cores were not found to exhibit systematic patterns with distance down-lake (Figure 4, C). The lowest OM values were observed in the Keithley Creek sub-basin which suggest higher levels of clastic sediment yield in this basin.

The results from particle size, laminae thickness, and percent organics suggest that sediment delivered from the main Cariboo River is the primary source of sediment to Cariboo Lake. Massive layering of sediment and coarse-grained particle sizes are limited to areas proximal to Pine Creek, Frank Creek and Keithley Creek deltas where localized turbidity currents are active. Outside of these areas, where turbidity currents and bedload transport processes are reduced, the sediment in Cariboo Lake is largely comprised of rhythmically laminated silt and clay sediments likely transported primarily through suspended sediment processes from the main Cariboo River. In the Keithley Creek sub-basin grain size and laminae structures are larger in size than those observed in the main Cariboo River basin suggesting local sediment inputs from the Keithley Creek are significant (Figure 5, C).

4.3 Sediment Accumulation Chronology

Four vibra sediment cores, ranging from 2 – 4 m in length, were retrieved from the deepest portions of Cariboo Lake (Figure 2). Cores V1 (2.9 m) and V2 (3.8 m) in the main Cariboo River basin were selected for detailed analysis as these two cores had organic material for AMS radiocarbon dating, and their sedimentary record was well preserved. The chronology of the two cores is provided by a small number of AMS radiocarbon dates and laminae counting. No evidence of volcanic tephra was found within either of the two cores. Westgate (1977) reports the most recent major volcanic ash event to reach central BC occurred 2100 yr BP, predating the basal age of the four sediment cores. This combined with the dark colour of the clastic core sediments

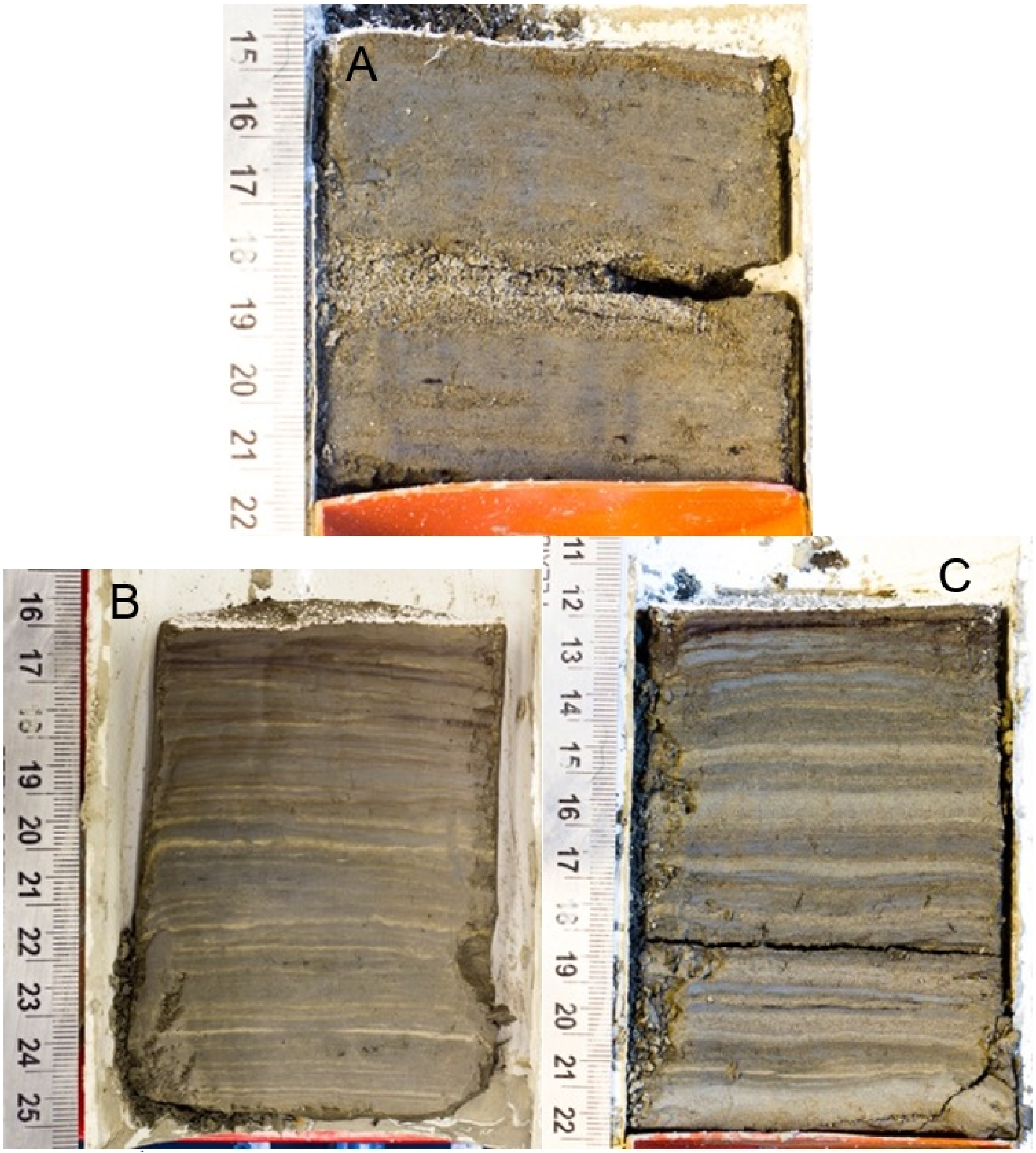

Figure 5: Selected surficial Ekman sediment core photographs. A (E1) is proximal to the Cariboo River delta (0.3 km down lake). B (E13) was retrieved from the second deepest basin in the lake in the Cariboo River basin (5.24 km down lake). C (E18) was retrieved from the Keithley Creek sub-basin (29.53 km down lake).

prevented finding smaller volcanic ash events within the cores. Records of grain size, varve thickness, and organic content from these two cores demonstrate patterns in sediment delivery to Cariboo Lake over the past 2000 years.

4.3.1 Chronology

Organic material for dating in the clastic dominated cores was extremely limited. AMS radiocarbon dates obtained for cores V1 and V2 provide limited temporal control and evidence of sediment accumulation rates. A small twig from V1 at 347 cm yielded a date of 1899-1819 cal BP. Two separate samples were analyzed from V2, one comprised of a large twig at 222 cm yielding a date of 490-316 cal BP (V2a), and a combination of two separate organic pieces which were combined into one sample, a twig at 286 cm and a pine needle at 294 cm, providing a date of 2045-1895 cal BP (V2b). Figure 6 shows the dating calibration curves derived for the three AMS radiocarbon dates and accumulation rates from couplet thickness counting of Ekman surficial cores 13-15. The dates from samples V1 and V2b yield consistent accumulation rates of 1.87 +/- 0.04 mm/yr and 1.47 +/- 0.11 mm/yr respectively. AMS sample V2a yields an accumulation rate of 5.51 mm/yr inconsistent with the rates provided for V1 and V2b.

Ekman surficial cores 13-15, shown in Figure 6, are proximal to the V2 long core (see Figure 2). The light-dark couplets in the short cores are identical to annual deposits noted in dozens of other lakes throughout BC (e.g. Hodder et al., 2007) so it is assumed that they closely approximate varves, in which case they exhibit accumulation rates of 2.24, 2.52, and 2.31 mm/yr respectively. Higher accumulation rates are expected for the Ekman samples as they are not subjected to the same level of compaction as is deeper sediment in the long cores. The consistency of the E13-E15 inferred accumulation rates when compared with two of the AMS dates from the V1 and V2b cores (Figure 6) are additional compelling evidence of the varved nature of the sediment record. This consistency also suggests that the V2a AMS sample is suspect for temporal control. In viewing the V2a sample orientation and position along the outer core it is speculated that the sample may have been pulled down during the coring process due to the large twig size at about 4 cm. This probably results in the erroneously high accumulation rate for V2a.

Accumulation rates in areas proximal to river inputs in nearby Quesnel Lake were measured to be about 0.72 mm/a (see Figure 9 in Gilbert and Desloges, 2012). Sediment inputs are expected to be lower in Quesnel Lake compared to Cariboo Lake, with more arid and less glaciated portions of the Quesnel Lake watershed contributing to that lower rate. Accumulation rates of 1.47 to 1.87 mm are consistent for a smaller Cariboo Lake watershed with a higher fraction of glacier cover. Laminae couplet thickness in Ekmans and two of the three vibra core AMS dates do not support the V2a accumulation rate of 5.51 mm/yr and therefore it was not included in subsequent analysis. The AMS radiocarbon dates from samples V1 and V2b provide an important control when interpreting the inferred temporal pattern of sediment inputs to Cariboo Lake. The top section of cores V1 and V2 were disturbed during coring - 110 mm for V1 and 70 mm for V2. While the Ekman cores were too short to overlap with the undisturbed sections of the vibra cores, laminae thickness similarities shown in Figure 6, allow anchoring the top of core dates to 0/0 (depth/date).

Three distinct sediment facies were observed in both V1 and V2: discernible couplets, indiscernible couplets (disturbed facies) and graded turbidite events. The similarity in couplet structure and thickness between cores V1 and V2 strongly suggested these are varves. This interpretation is supported by the two valid AMS radiocarbon dated samples from cores V1 and V2 which corresponded reasonably well with the couplet count chronology at the same depth. A small difference between the two chronologies is present due to some isolated disturbed sections of core, core compaction, undercounting, and subjectivity in classifying the occasionally thicker (4 to 47 mm thick) graded to massive laminae/beds.

Laminae/beds with D_{50} grain size greater than 3 standard deviations from the mean were classified as event-based turbidite beds. Laminae with thickness greater than 6 standard deviations for V1 and 2 standard deviations for V2 from the mean were classified as event-based turbidite beds. Figure 7 examples show the difference in regular laminae compared to an event-based turbidite bed. Turbidite beds observed in V1 and V2 were well defined and graded (see Figure 7, d). These turbidite beds are similar in structure to those described in Sabatier et al. (2022) as originating from a flood, glacial lake outburst flood, or delta collapse

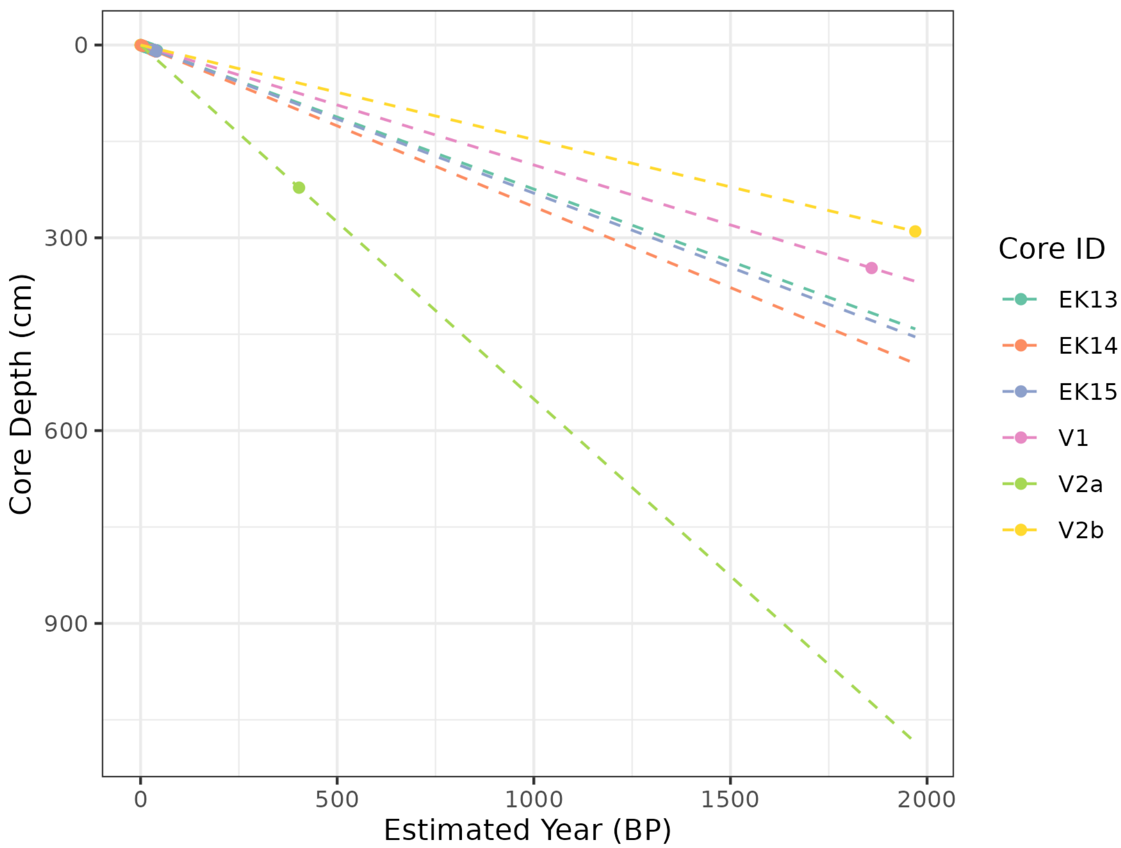

Figure 6: Cumulative accumulation rates for cores V1 and V2 using AMS dates V1, V2a and V2b and extrapolation of observed Ekman surficial core couplet thicknesses in E13, E14, and E15 all three of which are proximal to V2.

event. Since the Cariboo River upstream of Cariboo Lake is filtered by headwater proglacial lakes, it is more likely the turbidite beds at the distal V1 and V2 site are from localized sidewall tributary floods. Collapse of the foreslope of an oversteppened Cariboo delta is also possible.

Where possible the thickness, grain size statistics, and percent organic matter (OM) were analyzed for each event layer. The turbidite bed grain size, OM, and thickness shown in Table 1 illustrate the high sediment flux during these events compared to the regular, annually occurring couplets. The composition of sediment grains within the event-based layers were all characterized by a coarser single mode with less than 0.01% clay, over 98% silt and less than 1% sand. The grain size distribution for the regular couplet sediments is characterized by a bi-modal distribution with an average composition of 16% clay, 83% silt, and less than 1% sand. Figure 8 shows that some event layers are coincident in time between V1 and V2. Since each of the event-based layers contain sediment deposited over a single, potentially localized event, they were removed from subsequent trend analyses of varve thickness, grain size, and percent organics. After removal, the long core sediment records are thought to be most representative of watershed wide trends in river discharge influenced by temperature and precipitation rather than isolated events and inputs from nearby tributaries and hillslopes.

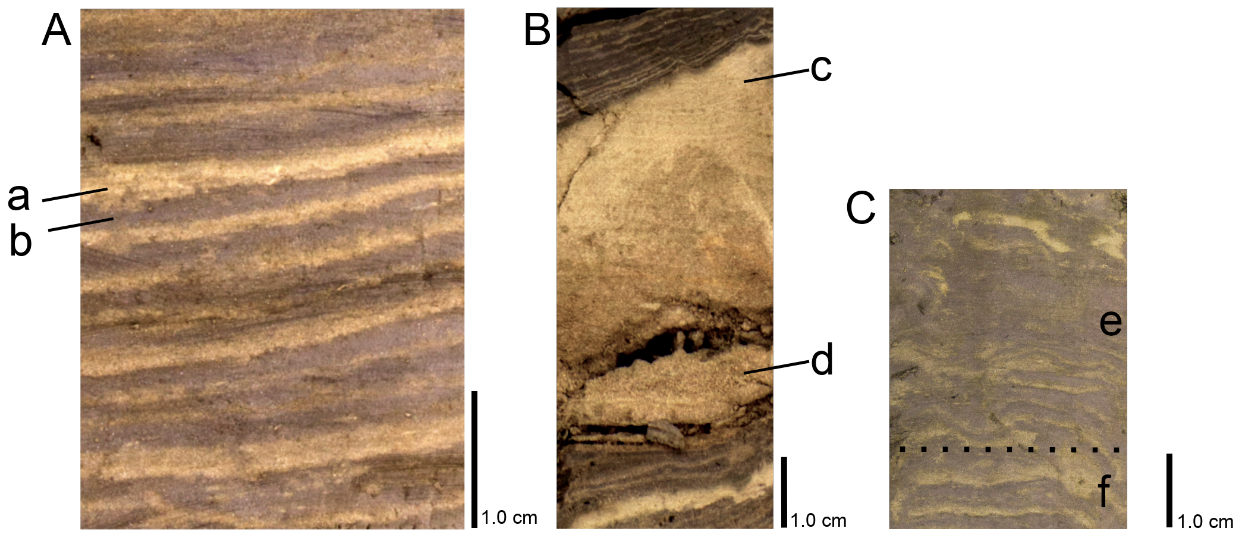

Figure 7: A. Example of regular laminae from V1 at a depth of 360 cm. B. an event-based turbidite bed from V2 at a depth of 230 cm. Features labeled within this figure include: ‘a’ high flow spring/summer freshet laminae, ‘b’ low flow winter laminae, ‘c’ top of the turbidite bed, and ‘d’ the bottom of the turbidite bed. C. shows massive beds ‘e’ over more distict laminations ‘f’.

Table 1: Sediment characteristics of regular laminae 'Couplet (varve)' compared to couplets classified as turbidite beds 'Events' for V1 and V2. The 'Couplet (varve)' is the mean sediment characteristic for all regular laminae couplets. The 'Event mean' is the mean sediment characteristic value for couplets classified as events, 'Event sd' is the standard deviation, and 'Event n' is the number of turbidite beds

core	metric	Couplet (varve) mean	Event mean	Event sd	Event n
V1	D_{50} (µm)	7.64	9.68	0.80	5
V2	D_{50} (µm)	6.35	16.20	9.40	6
V1	OM (%)	4.75	4.67	0.53	3
V2	OM (%)	4.71	2.86	0.94	4
V1	Avg. Thickness (mm)	2.40	10.32	4.24	5

core	metric	Couplet (varve) mean	Event mean	Event sd	Event n
V2	Avg. Thickness (mm)	1.51	11.17	15.89	7

The varve-based chronology is based on the counting of discernible couplets with graded turbidite facies removed. The absence of laminae couplets in the disturbed-massive units makes interpreting the time elapsed over each of these units difficult (see Figure 7 C). To compensate for the depth intervals associated with the disturbed sections, a 30-year moving average of sediment accumulation rates from immediately above and below the disturbed sections were used to interpolate accumulation rates over each facies (see method described in Menounos et al., 2008). For core V1, laminae couplets were counted down to a core depth of 347 cm, where the AMS radiocarbon organic material was retrieved. This resulted in a V1 couplet-derived age estimated of 1450 BP compared to the AMS radiocarbon estimate of 1899 - 1819 cal BP. For core V2 a date of 1886 BP was estimated by couplet counting down to a core depth of 294 cm which matches more closely with the V2b AMS radiocarbon date of 2045-1895 cal BP. The better alignment between the couplet counting age and the AMS derived age in V2 can be attributed to the higher degree of core disturbance in V1 compared to V2. Disturbed sections that had indiscernible couplets may have resulted in the undercounting within core V1. Still, based on the relatively close agreement between the AMS radiocarbon dated organic material and couplet counting, laminae couplets in V1 and V2 are considered to be deposited annually. Close alignment was not expected due to the aforementioned errors present in the couplet counting methodology and the limited 14C dates available.

The basal age for each core is estimated using both the varve chronology and the AMS radiocarbon accumulation rate. The basal age of V1 at a depth of 382 cm is approximately 1620 BP based on the varve chronology and 2046 cal BP based on the extrapolated 14C date. The basal age of V2 at a depth of 291 cm is about 1910 BP based on the varve chronology and 2007 cal BP by extrapolating the 14C. Accumulation rates estimated using the varve counting chronology and the AMS radiocarbon date chronology had a larger difference at V1 with 2.4 mm/yr and 1.87 +/- 0.04 mm/yr, respectively. Closer agreement was observed at V2 with 1.52 mm/yr estimated using the couplet counting method and 1.47 +/- 0.11 mm/yr from the AMS radiocarbon date. While V2 is likely the better predictor of changes in accumulation rates over the last 2000 years, we believe both cores are valid estimates of late Holocene sediment accumulation patterns in Cariboo Lake.

4.3.2 Sediment Accumulation Chronology and Statistics

For the laminae couplet time series, shown in Figure 9, only the discernible couplets are analyzed, event-based turbidites have been removed and disturbed facies are represented as gaps. The chronologies for this time series were derived using a linear interpolation from the AMS radiocarbon dates. The mean varve thickness for V1 is 2.4 mm and for V2 is 1.5 mm. Thicker varves are expected at V1 due to its closer proximity to the Cariboo River delta. This is also supported by the thicker varves observed in core E11 (proximal to V1) compared to E13 (proximal to V2) of 2.8 mm to 2.0 mm respectively. Figure 9 shows the time series of varve thickness measured from V1 and V2 and illustrates trends in suspended sediment delivery to Cariboo Lake. The measured couplet thicknesses in the two cores are plotted as standardized departures to facilitate comparison between the two cores. In each plot a 30-year moving average with a 1-year time step is plotted in black to emphasize decadal to centennial patterns in accumulation rate departures. The 30-year average varve thickness remains above average from 0 to 750 CE, for both V1 and V2, with a stronger signal observed for V1 which is closer to the main Cariboo River outlet. Below average varve thickness is observed at both V1 and V2 from 750-1600 CE. After 1600 CE, trends in varve thickness between the two cores depart, with V2 above average during the Little Ice Age and V1 remains below average. Sub-centennial trends are not reported due to the coarse temporal control for both V1 and V2.

4.3.2.1 Grain Size The mean D_{50} grain size at V1 is 7.6 +/- 0.01 µm compared to 6.3 +/- 0.01 µm at V2. The larger grain size and varve thickness at V1 compared to V2 is consistent with the spatial trends

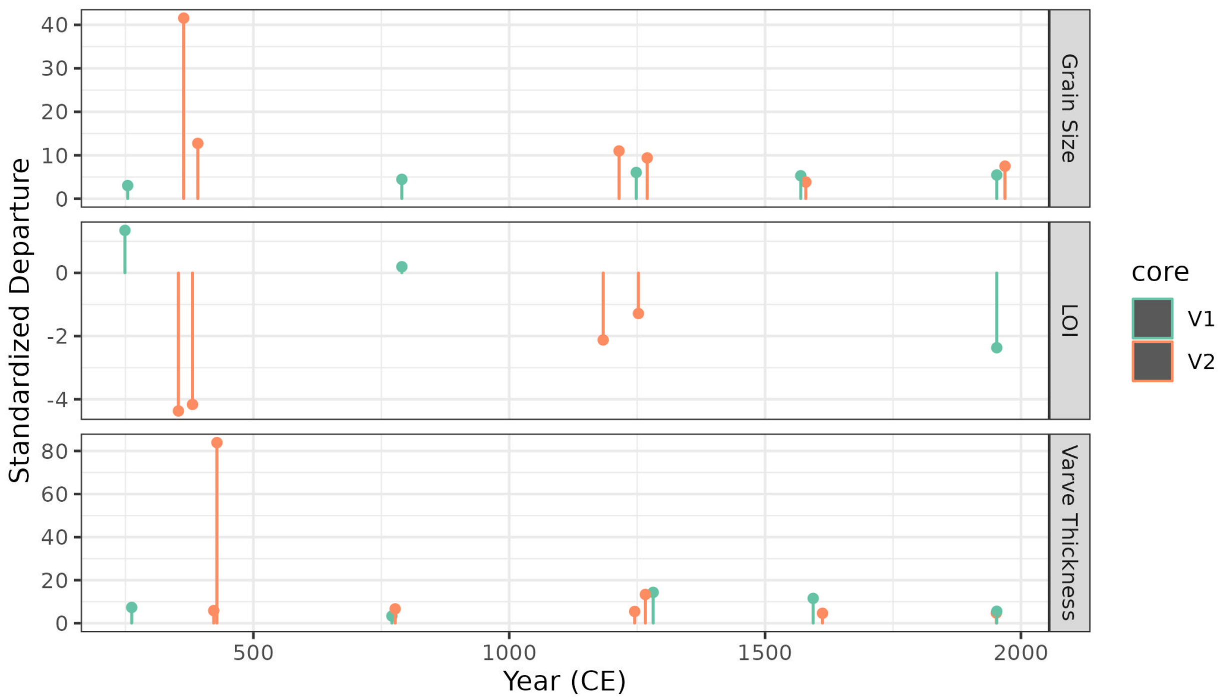

Figure 8: Timing and Standardized Departures of turbidite thickness, grain size, and OM for V1 and V2. Year (CE) is the estimated year using linear interpolation from the AMS radiocarbon dates.

in sediment delivery observed from the Ekman cores. While based on a limited number of measurements compared to the varve thickness analysis, the temporal pattern in standardized departures of D_{50} grain size between the two cores shows a consistent pattern (Figure 10). Both V1 and V2 have above average grain size between 0 to 700 CE and below average from 700 to 1500 CE. After 1500 CE, grain size follows an increasing trend with average to above average grain size. V1 shows a more dramatic increase in grain size compared to V2. While couplet thickness does not increase substantially over the LIA interval, gain size does. Overall, grain size fluctuations at a temporal resolution of about 100-years shows good correspondence between the two cores over the last 2000 years.

4.3.2.2 Organic Matter The whole core average OM content at V1 and V2 is similar at 4.76% and 4.80%, respectively, suggesting that the flux of allochthonous organic material to the core locations is not dependent on distance from the main Cariboo River as it is easily transported through the lake due to low density. This is also supported by the Ekman OM spatial analysis, where a systematic down-lake relationship was not observed (Figure 4, C). Figure 11 shows the percent organic matter (OM) for both V1 and V2. Higher levels of organic content are shown in V1 and V2 from 0-1000 CE and mostly below average from 1000-2000 CE. Specific periods of above average OM for V1 occur around CE 50-500, 650-1150, around 1300 and 1750-1850. OM in V2 matches above average values in the interval CE 250-550 and 650-950. During the last 100 years both cores show a persistent decline in OM which could be attributed to a relative increase in sediment delivery to Cariboo Lake suggested by the increase in D_{50} and varve thickness. As glaciers declined from peak LIA extents around 1750 CE, an increase in vegetation growth is expected which may also contribute to a decline in OM as organic content is locked up as needleleaf coniferous forest.

5 Discussion

Cariboo Lake was selected to test the utility of moderate sized glacier-fed lakes as archives of accessible long-term and high-resolution sedimentation input variability. Evidence of late Pleistocene deglaciation in

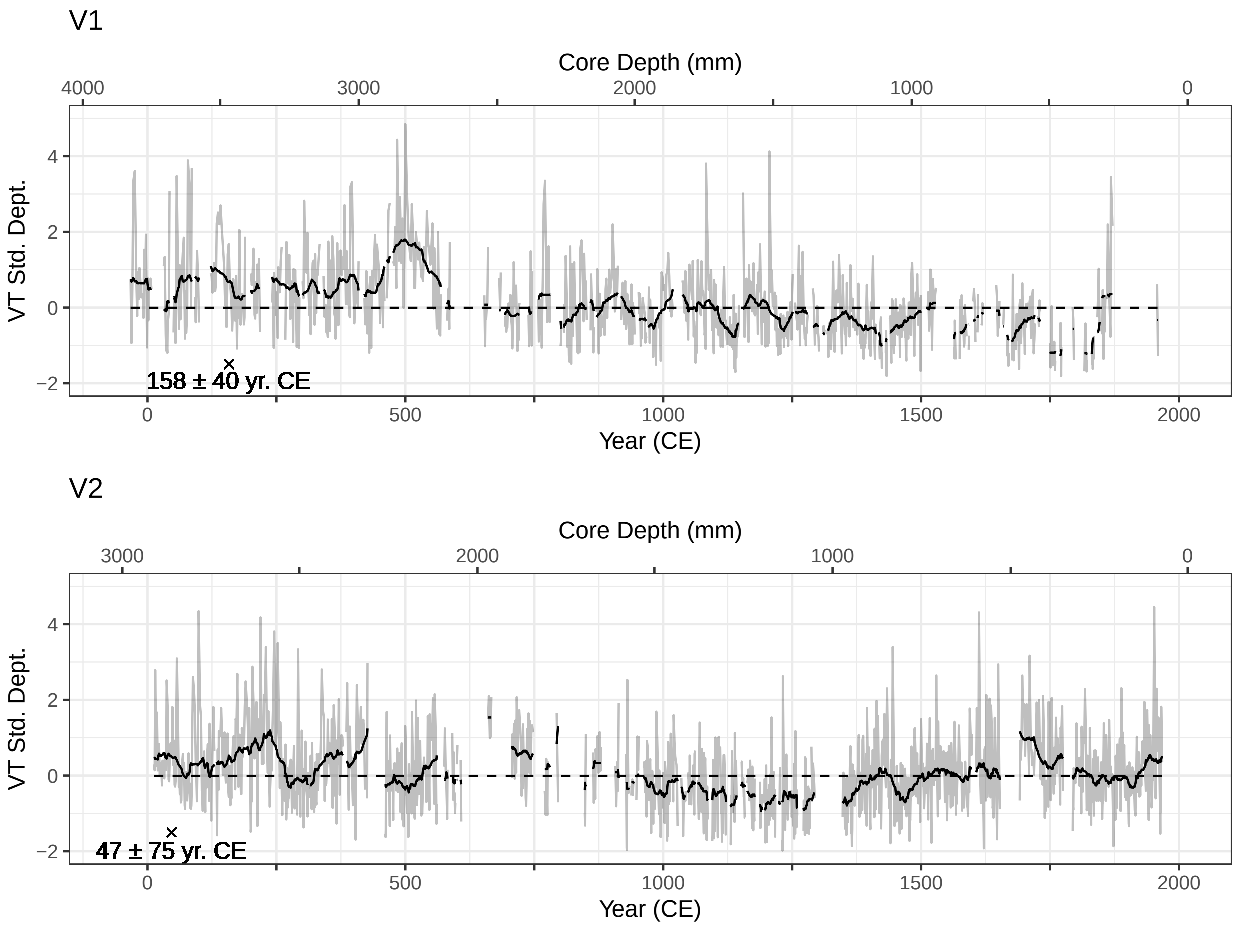

Figure 9: Standardized departure from the mean varve thickness (VT) for cores V1 and V2. Events are removed from the record and disturbed facies are shown as blank gaps in the record. The gap width of disturbed facies was calculated using a linear interpolation from the AMS radiocarbon dates. The gray lines represent measured varve thickness at couplet (annual) resolution where available, the black line is a 30-year moving average. Gaps correspond to portions of the core that did not have discernible varves. The bottom axes, labeled Year (CE), was estimated using linear interpolation from the AMS radiocarbon dates. Laminae counting in V1 was not possible beyond the estimated date of 1890 CE and beyond 1970 CE in V2. The black X's on the bottom graph of V1 and V2 denote the AMS radiocarbon age (± dating error) and depth of the respective sample.

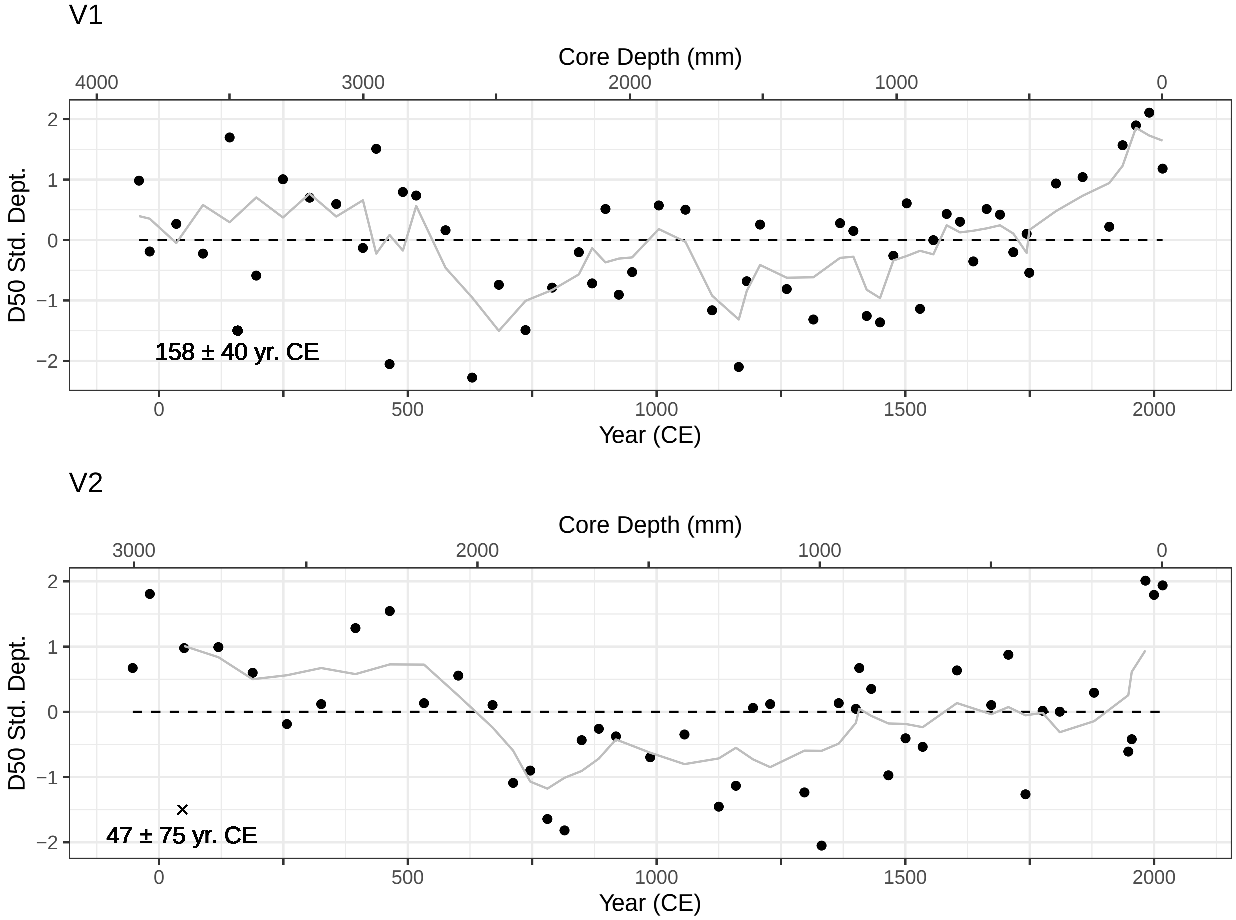

Figure 10: Standardized departure from the mean D 50 grain size for cores V1 and V2. The black points represent D 50 grain size at 5 - 10 cm intervals and the gray line is the 3 sample (125 year) moving average. The top axes, labeled Year (CE), was estimated using linear interpolation from the AMS radiocarbon dates. The black X's on the bottom graph of V1 and V2 denote the AMS radiocarbon age (± dating error) and depth of the respective sample.

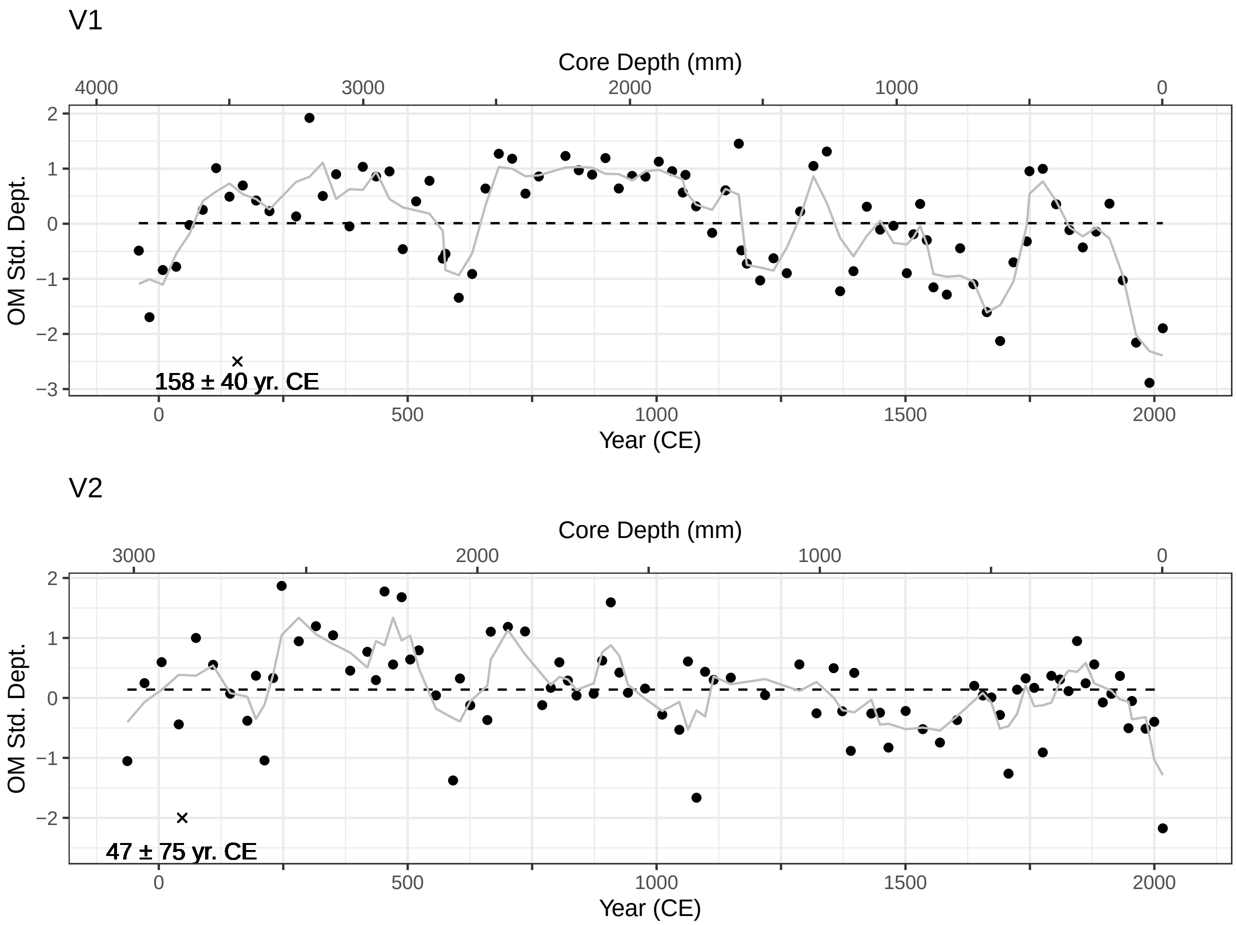

Figure 11: Standardized departure from the mean percent organic matter (OM) for cores V1 and V2. The black points represent percent OM at 2.5 - 5 cm intervals and the gray line is the 3 sample (75 year) moving average. The top axes, labelelled Year (CE), was estimated using linear interpolation from the AMS radiocarbon dates. The black X's on the bottom graph of V1 and V2 denote the AMS radiocarbon age (± dating error) and depth of the respective sample.

the Cariboo Lake region is provided by coarse temporal resolution sub-bottom acoustic results. A maximum deglacial sediment thickness of ~35 m puts Cariboo Lake in the middle to lower range of Holocene sediment inputs in Canadian Cordilleran lakes (see detailed discussion in Gilbert and Desloges, 2012). The study of smaller Mud Lake, in the Rocky Mountains to the east of Cariboo Lake (Figure 1 – inset) was evaluated by Hodder et al. (2006), who found the early phases of deglaciation and lake sediment infill started just prior to 9.6 ka BP. Gilbert and Desloges (2012) indicate deglaciation of the north and west arms of nearby Quesnel Lake was likely complete by 8.6 ka BP. Menounos et al. (2009) pointed to the deglaciation of most of the Cordilleran ice sheet before 10.5 ka BP. The Cariboo Lake acoustic results contribute to this regional record however the inferred bottom dates present uncertainty in the actual timing.

Unlike many other deglacial sediment packages in Canadian Cordilleran lakes, the sediment infill in Cariboo Lake has been subject to deep trenching during deglaciation and the early Holocene (Figure 3c). The troughs, with sediment infills occurring at different times, suggest the presence of highly erosive but intermittent bottom currents during deglaciation and into the very earliest Holocene. Energetic flow of cold sediment-rich meltwater flow would be required suggesting proximity of an actively retreating valley glacier. The absence of lower elevations moraines in the valley upstream of Cariboo Lake might indicate rapidly retreating ice into headwater locations. However, in general, moraines indicative of stagnant ice fronts in lower elevation settings are not common elsewhere throughout much of the eastern Cordillera suggesting that valley glacier development was limited.

High accumulation rates in contemporary ice-proximal lakes with extensive coverage of active glaciers have been observed to be between 0.5 m/a (Crookshanks and Gilbert, 2008) and as high as 1 m/a (Gilbert et al., 1997). Similar high accumulation rates in the late-glacial are inferred to have occurred in Quesnel Lake (Gilbert and Desloges, 2012), resulting in a thick pre-Holocene sediment package. This evidence for high pre/early Holocene accumulation rates in Quesnel Lake from large dynamic glaciers suggests that high accumulation rates are also likely for Cariboo Lake during this time.

Warming in the early Holocene, around 9.10-6.70 ka BP in the Rockies, specifically, (Luckman, 1986) and British Columbia, generally, (Clague, 1989) led to two possible sedimentation regimes. Where glaciers persist through the warm period resulting in more regular seasonality of sediment inputs and laminae couplet formation (e.g. Mud Lake, Hodder et al., 2006) and where glaciers disappear during the warm period, leading to much lower accumulation and seasonality (e.g. Moose Lake, Desloges, 1999).

Sub-bottom acoustic records from Transect B shown in Figure 3, which is proximal to the V1 core, indicate an upward transition from massive-unlayered (Facies A) to well-layered sediments (Facies B) at a depth of about 20 m. Assuming a maximum Holocene sediment accumulation rate of approximate 1.9 mm/yr from V1, this would put this transition at about 10.5 ka BP. The massive structure of Facies A is inferred to be due to high rates of sediment delivery as glaciers retreated upvalley during the early Holocene after the formation of the deep trenches. The well-layered sediment of Facies B, along with the continuation of laminae couplets observed in cores V1 and V2 over the last 2 ka, suggests that glaciers reduced in extent at the start of the Holocene but did not disappear completely. It is possible during this transition from Facies A to B, glaciers retreated above Lanezi Lake resulting in a more sediment filtering and thus a reduction in sediment delivery and the beginning of seasonally derived laminae couplet formation within Cariboo Lake.

Transect C, shown in Figure 3 is located in-between cores V1 and V2, has ~15 m of well layered sediment overlying a massive unlayered lower Facies A. Using a combined V1 and V2 average Holocene sediment accumulation rate of 1.7 mm/yr in this region of the lake, puts the transition from Facies A to B at around 9 ka BP, slightly later than the Transect B estimate. If sediment delivery was less prior to the Neoglacial, the estimated basal ages here would be much older. The timing of this transition is similar to the onset of deglaciation and start of the Holocene sediment package within Mud Lake, BC (Hodder et al., 2006) around 9.6 ka BP, at Moose Lake, BC (Desloges, 1999) around 10.3 ka BP, at Quesnel Lake, BC (Gilbert and Desloges, 2012) around 8.6 ka BP, and at the Upper Bow River, AB (Leonard and Reasoner, 1999) around 11.7 ka BP.

Higher resolution AMS dated sediments from the much thinner sediment package in the west arm of Quesnel Lake, located in the Cariboo Mountains (Figure 1), showed a very consistent mean rate of sedimentation throughout the entire Holocene (Gilbert and Desloges, 2012). Contrasting somewhat from this pattern are results from Menounos et al. (2009) and Desloges (1999) who note that early to mid-Holocene sediment accumulation rates in the southeastern Canadian Cordillera were lower than the late-Holocene Neoglacial period. However, those shifts come from watersheds with much higher percentages of glacier ice cover (~15-40%) coupled with the probable disappearance of glaciers during the warmer hypsithermal. So, any extrapolation of timing to the early sediment record of Cariboo Lake remains speculative.

Sediment inputs to Cariboo Lake are mainly delivered via the Cariboo River delta and thus changes in watershed-wide temperature and precipitation trends would be important. In contrast, inputs of sediment from the small tributary watersheds that boarder Cariboo Lake are controlled by more localized, watershed-specific responses. Although coarser grained sediments from discrete turbidite flows are found proximal to sidewall tributary deltas (Figure 4), they are only transferred to deep lake deposits during episodic events (Figure 8). The long core (V1 and V2) sediment is composed of nearly 99% silt and clay resulting in laminae couplets that are inferred to have been delivered via suspended sediment from the main Cariboo River. Therefore, trends observed in sediment accumulation at cores V1 and V2 likely best represent waterside-wide climate and glacier activity. While cores V1 and V2 do not produce identical results, it is likely the sediment yield data from these cores are within the range of 7-21% error, as reported in Evans and Church (2000) for other alpine lakes in British Columbia. The inferred error of cores V1 and V2 is attributed to the spatial heterogeneity of sediment accumulation across the Cariboo Lake, and is likely on the lower end of this error range due to its simple basin morphology. Retrieving more than two good long core sedimentary sequences, could have provided a better estimate in the error of sediment accumulation, however, the logistical demands of retrieving more cores prevented this. The Cariboo River has two main tributaries, the Upper Cariboo River and the Matthew River which are connected to high alpine peaks and glaciers providing a significant source of sediment (see Figure 2). Lanezi, Sandy and Ghost lakes act as sediment traps eliminating the transfer of coarse sediment and limiting the transfer of finer sediment from the glacier sediment production zones. This results in sediment accumulation rates that are on the low-end for the southeastern Cordillera (Hodder et al., 2006). Although connectivity is limited, there are sufficient seasonal contrasts in suspended sediment flux to produce couplets (annual varves) in the main basin of Cariboo Lake. This is unlike the west arm of Quesnel Lake where sediment rates are 2 to 3 times lower due to significant storage in the much larger upper watershed.

There is a documented range of late Holocene clastic sediment accumulation rates in glacier-fed lakes from across the Canadian Cordillera. Highest rates of > 2 cm/yr are observed in ice-contact to ice-proximal lakes of various sizes (Crookshanks and Gilbert, 2008; Desloges and Gilbert, 1994), to relatively low rates of < 1 mm/yr (Gilbert and Desloges, 2012). The range in accumulation rates has been understood to be a result in the variability of sediment production from glacier processes, the steepness of topography (Ballantyne, 2002), the persistence of ice cover and the degree of basin connectivity enhancing or impeding delivery of sediment down valley (Wohl et al., 2019). The average accumulation rate for Cariboo Lake of 1.7 mm/yr over the last two millennia is ideal for yielding discernible higher-resolution trends in sediment delivery over the late Holocene. The combination of upper watershed area, intervening storage, glacier cover and lake size are considered optimal during this period.

Actual lake sediment chronologies typically vary in their sensitivity to regional fluctuations in temperature and precipitation, from annual resolution in lakes with higher accumulation rates (e.g. Menounos and Clague, 2008) to only being able to resolve centennial-scale or lower resolution in lakes with low accumulation rates (e.g. Desloges, 1999). For the last 2000 years, the Cariboo Lake record is very high resolution. Figure 12a shows the (inferred) varve thickness chronology reconstructed as standardized departures from cores V1 and V2. There is a significant amount of noise in the record, typical of a filtered sediment transport system (e.g. Jerolmack and Paola, 2010), so a lower resolution 30-year moving average is superimposed on the raw couplet thickness data in Figure 12a. Figure 12b and 12c show the lower-resolution temporal patterns in D_{50} grain size and organic matter content, respectively. These trends are compared against the Moberg et al. (2005) regional climate proxy re-analysis for the northern hemisphere (Figure 12d), Solomina et al. (2016) western Canada peak glacier extent estimates (Figure 12e), and Ljungqvist et al. (2016) hydroclimate anomaly estimates for the northern hemisphere (Figure 12f). Most of these are at resolutions of centennial scale or lower.

For Cariboo Lake, above average varve thickness, grain size, and organic matter are observed for both V1 and

V2 from 0-700 CE which is coincident with the peak extent of the first millennial glacier advance (Solomina et al., 2016), and below average temperatures in the Northern Hemisphere (Ljungqvist et al., 2016). While above average grain size and varve thickness are expected during a time of increased glacier extent due to higher rates of sediment production and delivery. Above average organic matter could be explained by some contribution of increased soil erosion below treeline during a time of higher precipitation rates and subsequent high spring freshet flows. As temperatures warmed following the first millennial advance from 700-1200 CE into the Medieval Warm Period, a decline in varve thickness and grain size is observed while organic matter remains high during a warmer and dryer climate. Over the Little Ice Age, varves are thicker and coarser, and organic matter content remains average to below average as glaciers advance in a colder and wetter climate. Following the LIA, a dramatic decline in organic matter is observed coincident with above average grain size suggestive of high magnitude clastic sediment delivery. The response of Cariboo Lake sediment accumulation appears to be more sensitive (higher variability in the original standardized departures of varve thickness) to glacier activity during the LIA compared to previous advances around 500 CE and 1200-1500 CE. There is some evidence for a rapid increase in grain size and reduction in OM content in the 20^{th} century portion of the record. It is tempting to conclude that 20^{th} century warming in the main cause. However, hydraulic mining practices during the Cariboo Gold Rush and deforestation began during the late 1800s and may have contributed to these anomalies.

6 Conclusions

The moderated-sized Cariboo Lake provides a very good record of deglacial and Holocene sediment inputs. The steep climatic gradient from the wetter, glacier covered, headwaters to the semi-arid, lower elevation zones of the lake, result in sediment input via the main Cariboo Lake delta that is predominately derived from the glacier production zone. This conclusion is supported by the down-lake trends observed in grain-size and organic matter content. The smaller alluvial-fan deltas from side tributaries appear to be paraglacial relic features, similar to those described in Church and Ryder (1972), and likely formed during deglaciation and the earliest Holocene as no evidence of significant inputs during the Holocene were found in this study.

1. Sub-bottom acoustic records provide a coarse temporal resolution chronology of early and mid-Holocene sediment accumulation. The transition of massive to well-layered sediments occurs around 10.5 to 9 ka BP. This is similar to other lakes in the region suggesting fairly consistent and rapid withdrawal of valley-bottom glacier ice into the highest elevation zones.
2. There are still limitations in the ability to retrieve sufficiently long cores (> 10-15 m), that would provide a high resolution record of sediment inputs over the entire Holocene. If trends observed in other southern Canadian Cordilleran lakes prevail, the early and mid-Holocene input of sediment during the hypsithermal would have been significantly reduced resulting in a Holocene sediment package within the 10-15 m range. Acoustic Facies B most likely represents this unit.
3. Sedimentary structures in the long cores indicated sediment delivery over the late Holocene to present is dominated by overflow currents of silt (spring freshet) and clay (winter settling) resulting in the formation of rhythmically laminated couplets that are mainly varves. While there is relatively close agreement between sediment chronology from laminae counting and the two AMS dates, it is not possible to develop a chronology that provides a precisely dated sediment yield record over the last 2 ka. However, the observed mean accumulation rate (1.7 mm/yr), the variance in accumulation rate and the low-frequency trends are important indicators of late Holocene environmental change.
4. Periods of peak glacier extent, such as during the First Millennial Advance (~ 200 to 700 CE) and Little Ice Age (~1600 to 1900 CE) are correlated with thicker and coarser varves in Cariboo Lake. We conclude that sediment accumulation in Cariboo Lake was more sensitive to glacier activity during the LIA compared to earlier advances. Trends in organic matter content appear to be less correlated with watershed sediment delivery and may be more sensitive to vegetation changes in the basin.
5. Trends in sediment characteristics after 1860 CE may be related to climate warming following the LIA. However, there are complications in this watershed via large-scale mining proximal to the lake and some upper watershed deforestation. They also may have been contributing factors to an increase in sediment delivery to the lake.

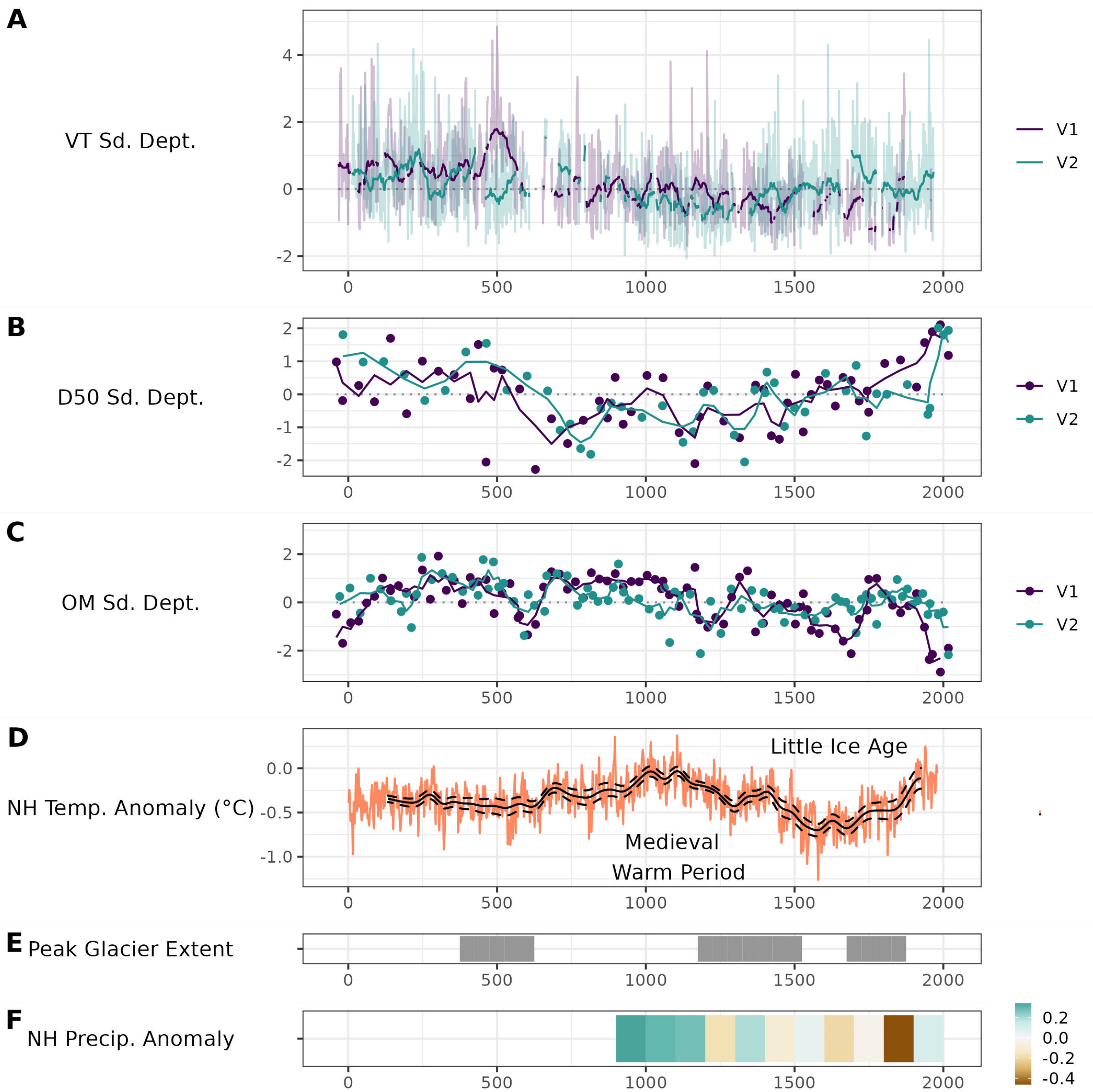

Figure 12: Cariboo Lake sediment characteristics for cores V1 (purple) and V2 (green) and Northern Hemisphere (NH) climate proxies. A, is the standardized departure (Sd. Dept.) from the mean varve thickness (VT) for annual couplets (light colour) and 30-year moving average (dark lines). B, is the standardized departure from the mean D 50 grain size, the coloured dots represent D 50 grain size at 5 - 10 cm intervals and the coloured lines are the 3 sample (125 year) moving average. C, is the standardized departure from the mean percent organic matter (OM) for cores V1 and V2. The coloured dots represent percent OM at 2.5 - 5 cm intervals and the coloured lines are the 3 sample (75 year) moving average. D, Moberg, Sonechkin and Holmgren (2005) Nothern Hemisphere annual temperature anomaly from the 1961-1990 mean, the orange line is the full reconstruction from high and low frequency proxies, and the black line is the low frequency proxy component with upper and lower uncertainty marked by dashed blue lines. E, Solomina et al., (2016) periods of peak glacier extent in western Canada. F, Ljungqvist et al., (2016) Nothern Hemisphere hydroclimate variability, expressed as standardized unitless anomalies ranging from -2 to 2, relative to the centennial mean and standard deviation over the eleventh-nineteenth centuries (see methods for Fig. 5 in (Ljungqvist et al., 2016).

The average sediment accumulation rate of 1.7 mm/yr is ideal for yielding higher-resolution trends in sediment delivery over the last two millennia. Above average varve thickness and grain size is observed from 0 to 700 CE, below average from 700 to 1500 CE, and average to above average from 1500 CE to present. Trends in organic matter appear to be less correlated with watershed sediment delivery and may be more sensitive to vegetation changes in the basin.

7 Acknowledgements

We thank Michael Allchin, Laszlo Enyedy, and Caitlin Langford at the Quesnel River Research Centre for assistance in field. Brian Menounos kindly provided access to vibra-coring equipment. Mike Gorton, George Kretschmann, Anna Soleski and Selina Amaral provided assistance with lab analysis of sediment samples. Funding was provided by the University of Toronto.

References

Ballantyne CK (2002) Paraglacial geomorphology. *Quaternary science reviews* 21(18). OXFORD: Elsevier Ltd: 1935–2017.

Bolch T(submitter) and Bolch T(analyst) (2008) GLIMS Glacier Database. Boulder, CO: National Snow; Ice Data Center. Boulder, CO. DOI: 10.7265/N5V98602.

Church M and Ryder JM (1972) Paraglacial Sedimentation: A Consideration of Fluvial Processes Conditioned by Glaciation. *GSA Bulletin* 83(10): 3059–3072. DOI: 10.1130/0016-7606(1972)83[3059:PSACOF]2.0.CO;2.

Clague JJ (1989) Quaternary geology of the Canadian Cordillera. DOI: 10.1130/dnag-gna-k1.15.

Crookshanks S and Gilbert R (2008) Continuous, diurnally fluctuating turbidity currents in Kluane Lake, Yukon Territory. *Canadian journal of earth sciences* 45(10). National Research Council of Canada: 1123–1138.

Desloges JR (1999) Geomorphic and climatic interpretations of abrupt changes in glaciolacustrine deposition at Moose Lake, British Columbia, Canada. *Gff* 121(3): 202–207. DOI: 10.1080/11035899901213202.

Desloges JR and Gilbert R (1994) Sediment source and hydroclimatic inferences from glacial lake sediments: the postglacial sedimentary record of Lillooet Lake, British Columbia. *Journal of Hydrology* 159(1-4). Elsevier: 375–393. DOI: 10.1016/0022-1694(94)90268-2.

Dirszowsky RW and Desloges JR (1997) Glaciolacustrine sediments and neoglacial history of the Chephren lake basin, Banff National Park, Alberta. *Geographie Physique Et Quaternaire* 51(1): 41–53. DOI: 10.7202/004804ar.

Gilbert R and Desloges JR (2012) Late glacial and Holocene sedimentary environments of Quesnel Lake, British Columbia. *Geomorphology* 179. Elsevier B.V.: 186–196. DOI: 10.1016/j.geomorph.2012.08.010.

Gilbert R, Desloges JR and Clague JJ (1997) The glacilacustrine sedimentary environment of Bowser Lake in the northern Coast Mountains of British Columbia, Canada. *Journal of Paleolimnology* 17(3). Kluwer Academic Publishers: 333–348. DOI: 10.1023/A:1007900411724.

Gray AB, Pasternack GB and Watson EB (2010) Hydrogen peroxide treatment effects on the particle size distribution of alluvial and marsh sediments. *Holocene (Sevenoaks)* 20(2). London, England: SAGE Publications: 293–301.

Hodder KR, Desloges JR and Gilbert R (2006) Pattern and timing of sediment infill at glacier-fed Mud Lake: Implications for lateglacial and Holocene environments in the Monashee Mountain region of British Columbia, Canada. *Holocene* 16(5): 705–716. DOI: 10.1191/0959683606hl965rp.

Hodder KR, Gilbert R and Desloges JR (2007) Glaciolacustrine varved sediment as an alpine hydroclimatic proxy. *Journal of Paleolimnology* 38(3): 365–394. DOI: 10.1007/s10933-006-9083-9.

Huber M and Knutti R (2012) Anthropogenic and natural warming inferred from changes in Earth's energy balance. *Nature geoscience* 5(1). NEW YORK: Springer Nature: 31–36.

Jerolmack DJ and Paola C (2010) Shredding of environmental signals by sediment transport. *Geophysical research letters* 37(19). Jerolmack,. Washington, DC: Blackwell Publishing Ltd: n/a.

Leonard EM (1986) Use of lacustrine sedimentary sequences as indicators of Holocene glacial history, Banff National Park, Alberta, Canada. *Quaternary Research* 26(2): 218–231. DOI: 10.1016/0033-5894(86)90106-7.

Leonard EM and Reasoner MA (1999) A continuous holocene glacial record inferred from proglacial lake sediments in Banff National Park, Alberta, Canada. *Quaternary Research* 51(1). No longer published by Elsevier: 1–13. DOI: 10.1006/qres.1998.2009.

Ljungqvist FC, Krusic PJ, Sundqvist HS, et al. (2016) Northern hemisphere hydroclimate variability over the past twelve centuries. *Nature* 532: 94+. Available at: https://link.gale.com/apps/doc/A449108229/EAIM?u=usaskmain&sid=bookmark-EAIM&xid=1dfbd232.

Luckman BH (1986) Reconstruction of Little Ice Age Events in the Canadian Rocky Mountains. *Géographie physique et quaternaire* 40(1). Montréal, PQ: Les Presses de l'Université de Montréal: 17–28.

Masson-Delmotte V, Schulz M, Abe-Ouchi A, et al. (2013) Information from paleoclimate archives. In: Stocker TF, Qin D, Plattner G-K, et al. (eds) *Climate Change 2013: The Physical Science Basis. Contribution of Working Group i to the Fifth Assessment Report of the Intergovernmental Panel on Climate Change.* Cambridge, UK: Cambridge University Press, pp. 383–464. DOI: 10.1017/CBO9781107415324.013.

Menounos BP and Clague JJ (2008) Reconstructing hydro-climatic events and glacier fluctuations over the past millennium from annually laminated sediments of Cheakamus Lake, southern Coast Mountains, British Columbia, Canada. *Quaternary Science Reviews* 27(7-8): 701–713. DOI: 10.1016/j.quascirev.2008.01.007.

Menounos BP, Schiefer E and Slaymaker O (2006) Nested temporal suspended sediment yields, Green Lake Basin, British Columbia, Canada. *Geomorphology* 79(1-2): 114–129. DOI: 10.1016/j.geomorph.2005.09.020.

Menounos BP, Osborn GD, Clague JJ, et al. (2009) Latest Pleistocene and Holocene glacier fluctuations in western Canada. *Quaternary Science Reviews* 28(21-22): 2049–2074. DOI: 10.1016/j.quascirev.2008.10.018.

Moberg A, Sonechkin DM, Holmgren K, et al. (2005) Highly variable Northern Hemisphere temperatures reconstructed from low- and high-resolution proxy data. *Nature* 433(7026): 613–617. DOI: 10.1038/nature03265.

Nelson MC, Ingram SE, Dugmore AJ, et al. (2016) Climate challenges, vulnerabilities, and food security. *Proceedings of the National Academy of Sciences* 113(2): 298–303. DOI: 10.1073/pnas.1506494113.

Neukom R, Barboza LA, Erb MP, et al. (2019) Consistent multidecadal variability in global temperature reconstructions and simulations over the Common Era. *Nature geoscience* 12(8). PAGES 2k Consortium: 643–649.

Sabatier P, Moernaut J, Bertrand S, et al. (2022) A Review of Event Deposits in Lake Sediments. *Quaternary* 5(3). MDPI: 34. DOI: 10.3390/quat5030034.

Schneider CA, Rasband WS and Eliceiri KW (2012) NIH Image to ImageJ: 25 years of image analysis. *Nature Methods* 9(7): 671–675. DOI: 10.1038/nmeth.2089.

Smith JG (2003) Aspects of the loss-on-ignition (loi) technique in the context of clay-rich, glaciolacustrine sediments. *Geografiska Annaler: Series A, Physical Geography* 85(1). Wiley/Blackwell (10.1111): 91–97. DOI: 10.1111/1468-0459.00191.

Solomina ON, Bradley RS, Jomelli V, et al. (2016) Glacier fluctuations during the past 2000 years. *Quaternary Science Reviews* 149: 61–90. DOI: 10.1016/j.quascirev.2016.04.008.

Turney CSM, McGregor HV, Francus P, et al. (2019) Introduction to the special issue "climate of the past 2000 years: Regional and trans-regional syntheses". *Climate of the past* 15(2). Naturvetenskapliga fakulteten; Copernicus GmbH: 611–615.

Westgate JA (1977) Identification and Significance of Late Holocene Tephra From Otter Creek, Southern British Columbia, and Localities in West-Central Alberta. *Can J Earth Sci* 14(11): 2593–2600. DOI: 10.1139/e77-224.

Wohl E, Brierley G, Cadol D, et al. (2019) Connectivity as an emergent property of geomorphic systems. *Earth Surface Processes and Landforms* 44(1): 4–26. DOI: 10.1002/esp.4434.